13th World Conference on Earthquake Engineering
Vancouver, B.C., Canada
August 1-6, 2004
Paper No. 1458

MODELLING OF PLASTIC HINGES IN EXTERNALLY CONFINED REINFORCED CONCRETE COLUMNS

Munawar A. HUSSAIN[1] and Robert G. DRIVER[2]

SUMMARY

The external confinement of reinforced concrete columns by collars made from steel hollow structural sections (HSS) has proved to be a successful rehabilitation scheme for seismically deficient existing reinforced concrete frame buildings, as has been demonstrated through extensive experimental study conducted at the University of Alberta. The experimental programme consisted of two phases: in phase one, the behaviour of externally confined columns under concentric monotonic loading was studied and in phase two, the behaviour of externally confined columns under simulated seismic loading was studied. The first step in the modelling of plastic hinges is the development of a model to predict the material curves of externally confined concrete. In this paper, a confinement model is proposed that takes into account both the flexural and axial stiffnesses of the collars to predict the behaviour of externally confined columns under concentric monotonic axial loading. The model predictions show very good agreement with the experimental results of the columns tested in phase one. In addition, using the proposed model the confined concrete material curves for the columns tested in phase two were obtained which, in turn, were used to predict their moment–curvature and moment–lateral drift envelope curves. The predicted envelope curves show very good agreement with the experimentally obtained curves at low and moderate values of lateral drift. Currently, the predictions overestimate the capacity at high levels of lateral drift due to the lack of a failure criterion in the stress vs. strain model. The post-peak portion of the model is still under development.

INTRODUCTION

Structural failures due to the collapse of columns are generally more catastrophic than those due to the collapse of beams. Several disastrous structural failures in recent earthquakes have been attributed to the poor performance of the columns. The performance of the columns during strong ground shaking can be improved by enhancement in deformability, strength, and energy dissipation at the location of plastic hinges through confinement. During the last three decades, numerous experimental and analytical studies on the confinement of concrete have been reported; some studies were devoted to the confinement of concrete by conventional transverse reinforcement [1-11] and others were devoted to the confinement of concrete by composite materials [12-13]. The experimental studies reported by Iyengar *et al.* [1] were on small-scale specimens and those reported by Vallenas *et al.* [2], Sheikh and Uzumeri [3], Scott *et al.* [4],

[1] Doctoral Candidate, Dept. of Civil and Envir. Engineering, University of Alberta, Edmonton, Canada.
[2] Associate Professor, Dept. of Civil and Envir. Engineering, University of Alberta, Edmonton, Canada.

and Mander *et al.* [5] were on large-scale specimens, whereas the others [6-13] focused primarily on the development of confinement models.

The major difference between the confinement mechanism for conventional transverse steel reinforcement and for composite materials is the variability of the confining pressure through the axial load history. Passive confining pressure is assumed to be constant when the confining elements behave plastically, which is the case typical of conventional steel tie reinforcement near the ultimate column strength. Variable confining pressure is generated when the confining elements have high stiffness. This is typical of confinement provided by either composite materials or by steel that remains elastic for the majority of the axial load history. The characteristics of variable passive confining pressure depend on the axial and transverse behaviour of the concrete, which in turn depends on the amount and the stiffness of the confinement provided.

External confinement by simple bolted or welded collars made from steel hollow structural sections (HSS) has proved through extensive experimental study at the University of Alberta to be an effective seismic rehabilitation scheme for square and rectangular reinforced concrete columns. The experimental programme consisted of two phases: in phase one, the behaviour of externally confined columns (specimens C01 through C09) under concentric axial loading was studied and in phase two, the behaviour of externally confined columns (specimens CL1 through CL8) under simulated seismic loading was studied. The details of the experimental programme and the pertinent test results have been given in a companion paper by Hussain and Driver [14]. The existing confinement models, both for conventional rebar confinement [6-11] and confinement by composite materials [12-13], are unable to predict the behaviour of externally confined columns by HSS collars under concentric monotonic axial loading. In addition, these confinement models cannot take into account the initial active confining pressure due to the pre-stressing of bolts in the case of confinement by bolted HSS collars. Both the axial and flexural stiffnesses of the collars contribute significantly to the confining pressure under the collars [15]. Although the contribution of the flexural stiffness of conventional transverse hoop reinforcement on the efficiency of the confinement mechanism has been acknowledged by researchers [1, 6, 9], this parameter has not been explicitly included in the prevailing confinement models. Generally, these models are based on the test results of columns with conventional confinement reinforcement of small diameter bars having significant axial stiffness but small flexural stiffness. Therefore, the omission of this parameter from the confinement models has no adverse consequence on their performance if used for columns confined by conventional transverse reinforcement in which confinement pressure is contributed principally by the axial stiffness of the transverse reinforcement. However, their performance would be questionable if used for columns confined by elements with significant axial and flexural stiffness. The beneficial effects of the flexural stiffness of the confining elements on the behaviour of the confined concrete have been studied experimentally by Khaloo and Bozorgzadeh [16] and through finite element analysis by Hussain and Driver [15]. The contribution of the flexural stiffness of the confining elements to the efficiency of confinement has also been appreciated in seismic rehabilitation studies of corrugated steel plate jacketing [17] and partially stiffened steel plate jacketing [18].

There exists similarity between collar confinement and confinement by composite materials; in both cases the confining pressure under the collars varies during the axial load history of the columns. However, the confining pressure exerted by composite materials varies linearly and the confining pressure imposed by collars varies nonlinearly with the increase of lateral strain due to the dilation of concrete. It is also to be noted that the flexural stiffness of the composite materials is negligible as compared to the flexural stiffness of the HSS collars.

PROPOSED MODEL FOR CONFINEMENT OF CONCRETE

A new uniaxial model—which approximates a path-independent reversible process with no memory—for the confinement of concrete is described herein which takes into account both axial and flexural stiffness of the confining elements. The proposed procedure takes into account both active and passive confining pressure. In the following sections the assumptions, approximations, and derivations of the proposed confinement model are presented.

A typical reinforced concrete column with HSS collar confinement is shown in Figure 1(a). For simplicity, the discrete collars are not modelled individually but are assumed smeared over the height of the column equivalent to a continuous tube as shown in Figure 1(b). The equivalent tube is assumed made of an orthotropic material having zero stiffness in the direction of column axis. The flexural stiffness of the tube in the direction normal to the longitudinal axis of the column should match the total flexural stiffness of all collars, over the height of the column, in the same direction. A similar argument applies to the axial stiffness of the equivalent tube and discrete collars. It is further assumed that the column with equivalent tube confinement expands uniformly over its height without bulging. Similar assumptions have been made by Légeron and Paultre [10] in the development of their confinement model for normal- and high-strength concrete, and by Caner and Bažant [19] while applying their computational model with smeared confinement to columns confined by spiral reinforcement. The equivalent confining tube is not shown in Figures 1(c) and 1(d) for clarity.

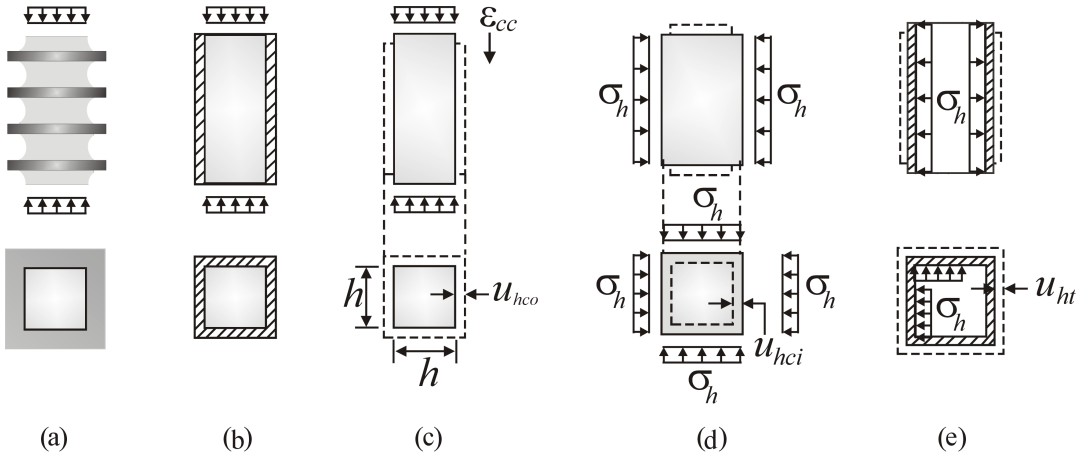

Figure 1: Discrete and smeared collars on a concrete prism under different stresses

Lateral Displacement Compatibility

Lateral displacement compatibility at the interface between the concrete prism and the confining tube is used to formulate the interaction between them. Consider the concrete column with square cross-section shown in Figure 1(c). When an axial strain ε_{cc} is applied to the concrete column, it is assumed that free uniform lateral expansion of the concrete takes place over the height and width of the column. As the prism is free to expand laterally, the lateral displacement u_{hco} can be evaluated as:

$$u_{hco} = \frac{\nu_c h \varepsilon_{cc}}{2} \qquad [1]$$

where ν_c is the Poisson's ratio; and h is the lateral dimension of the square concrete prism.

When the expansion of the concrete takes place due to the Poisson's effect, the confining tube resists this expansion by developing confining pressure on the concrete column through its axial and flexural stiffness. For simplicity, it is assumed that the confining pressure under the tube is uniformly distributed along the height and width of the column. If the concrete prism is subjected to external uniform confining pressure σ_h, as shown in Figure 1(d), the inward displacement u_{hci} at any face of the column is determined using the formula given by Young [20]:

$$u_{hci} = \frac{1-\nu_c}{2E_c} h\sigma_h \qquad [2]$$

where E_c is the modulus of elasticity of the concrete.

Now consider the lateral expansion of the confining tube as shown in Figure 1(e). For equilibrium, the pressure from the concrete on the confining tube must be the same as the pressure applied by the tube on the concrete, i.e., σ_h. It is assumed that the outward pressure on the confining tube causes uniform expansion of the tube along the width and height of the column as shown in this figure. The outward displacement of any side of the confining tube is denoted by u_{ht}. The compatibility condition requires that the equivalent confining tube and the column concrete surface remain in contact throughout the axial load history. According to this condition, the lateral displacement of the confining tube u_{ht} and the net resultant lateral displacement of the concrete ($u_{hco} - u_{hci}$) should be equal, i.e.:

$$u_{ht} = u_{hco} - u_{hci} \qquad [3]$$

It is to be noted that there does not exist a closed form expression for the determination of u_{ht} for the equivalent confining tube. In order to determine this displacement, the confining behaviour of the tube is required. The behaviour of the confining tube may be determined by finite element analysis, the details of which are given subsequently, where it can be expressed in terms of confinement stress vs. lateral strain. The behavioural curves of the confining tube take into account its material properties as well as its flexural and axial stiffnesses. Figure 2 shows a typical relationship between the average confinement stress and average lateral strain for a typical confining tube. This curve is nonlinear and it starts from the origin. In the case of collars with bolted corner connections, some initial confining pressure may exist due to the pre-stressing force in bolts. The initial active confining pressure is treated separately. The confinement stress vs. lateral strain curves of the confining tube are used to determine the confined material curves for concrete confined externally by HSS collars using a procedure described later.

From Figure 2, the slope of the *i*th secant line $(E_{ct})_i$ is defined as:

$$(E_{ct})_i = \frac{(\sigma_{ct})_i}{(\varepsilon_l)_i} \qquad [4]$$

and the slope of a general secant line E_{ct} can be defined as:

$$E_{ct} = \frac{\sigma_{ct}}{\varepsilon_l} \quad [5]$$

where $(\sigma_{ct})_i$ and $(\varepsilon_l)_i$ are the confinement stress and lateral strain corresponding to the point of intersection of the *i*th secant line with the confining stress vs. lateral strain curve of the confining tube and σ_{ct} and ε_l are the confining stress and lateral strain corresponding to the point of intersection of a general secant line with the confining stress vs. lateral strain curve. Using Equation 5, the lateral displacement of a side of the confining tube can be calculated as:

$$u_{ht} = \frac{\sigma_h h}{2E_{ct}} \quad [6]$$

By substituting the expressions for u_{hco}, u_{hci}, and u_{ht} into Equation 3, the following expression for the unknown confining pressure, σ_h, is obtained:

$$\sigma_h = \frac{\nu_c \varepsilon_{cc}}{\frac{1}{E_{ct}} + \frac{1-\nu_c}{E_c}} \quad [7]$$

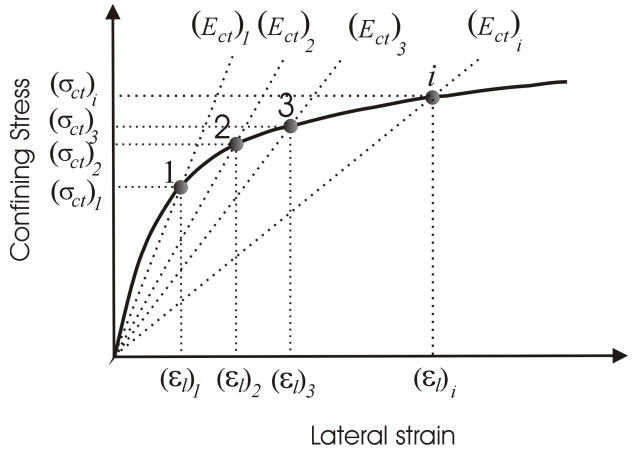

Figure 2: A typical confining stress vs. lateral strain curve

Confining Pressure vs. Lateral Strain Relationship

In conventional columns, the core is generally defined as the region enclosed by the centreline of the ties. Figures 3(a) and 3(b) show the ineffectively confined regions between tie levels and at the ties that are approximately parabolic in shape, as described by, for example, Sheikh and Uzumeri [7] and Mander *et al*. [8]. In the confinement model by Sheikh and Uzumeri [7], an expression for the strength enhancement factor was defined based on the core bounded by the centreline of the ties. It was assumed that the strength enhancement factor depends on the amount of transverse reinforcement, the stress in the transverse reinforcement at the peak strength of confined concrete, and the ratio of effectively confined concrete at the critical section to the core area bounded by the centreline of the ties, which in turn depends on the configuration and spacing of ties. Similarly, in the confinement model by Mander *et al.* [8], a confinement effectiveness coefficient was defined as the ratio of effectively confined concrete at the critical section to the concrete area in the core bounded by the centreline of the perimeter ties. The

average confining pressure was calculated assuming yielding of the transverse reinforcement at the peak stress of the confined concrete. The average confining pressures on the sides of the column were then multiplied by the confinement effectiveness coefficients to get the equivalent confining pressure. The peak stress of the confined concrete was then determined under this equivalent confining pressure. Saatcioglu and Razvi [9] also reported that the average confining pressure calculated by assuming yielding of the transverse reinforcement overestimates the confining pressure. A factor was therefore defined based on a regression analysis of experimental data to convert the average confining pressure to an equivalent confining pressure. The model proposed by Chung *et al.* [11] utilizes an effectively confined distance ratio instead of area to account for ineffectively confined regions in the core. The effectively confined distance ratio is defined as the ratio of the effectively confined width to the total width of the core concrete. This ratio takes the maximum value at the tie level and the minimum value at the critical section midway between two sets of ties. However, effectively and ineffectively confined regions were not dealt with separately. Instead, an expression for the strength enhancement factor was defined using regression in terms of the volumetric ratio of transverse steel, stress in the transverse steel at peak stress of the confined concrete, cylinder strength of the concrete, and effectively confined distance ratio.

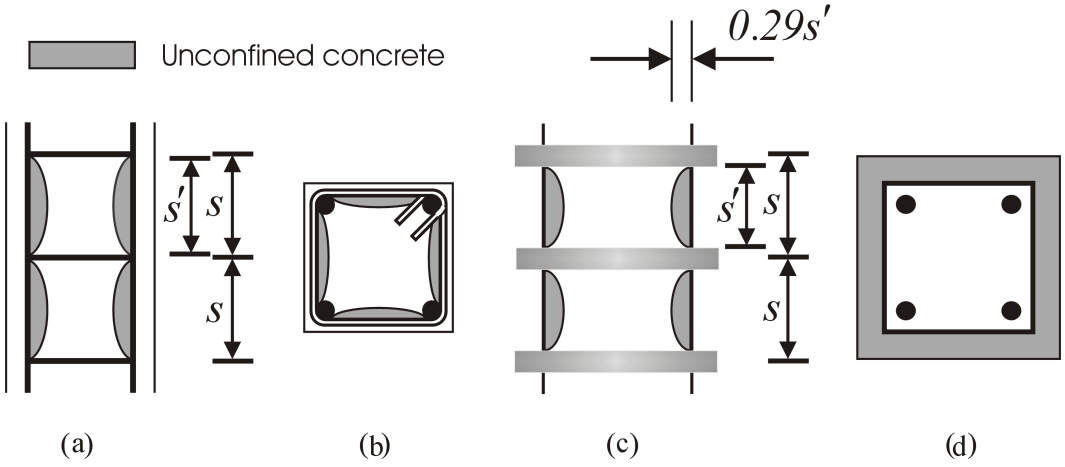

Figure 3: Unconfined concrete: (a) between tie levels; (b) at tie level; (c) between HSS collars; and (d) at HSS collar level (fully confined)

In contrast to the approaches described above wherein the ineffectively confined concrete is accounted for by a reduction factor, the proposed model for externally confined columns separates explicitly the behaviour of the effectively and ineffectively confined regions in the core. The core of the externally confined columns is equal to the gross dimensions of the columns. The load–strain curves of the effectively and ineffectively confined concrete regions in the core are defined, and are then combined to get the overall load–strain curve of the concrete in the core. The load–strain curves can be converted to stress–strain curves by dividing the load by the core area. Figure 3(c) shows the effectively and ineffectively confined regions between the collars and Figure 3(d) shows that there are no ineffectively confined regions at the collar level because of the considerable flexural stiffness of the sides of the collars, in addition to their axial stiffness. This assumption has been verified by both experimental and finite element studies. To model the behaviour of the effectively confined regions in the core, the collars are assumed smeared over the height of the columns, as described before, with confining pressure uniformly distributed on the side of the columns. The ineffectively confined concrete acts simply as a filler to transfer the confining force to the effectively confined regions. First, the behaviour of the

confined concrete in the core will be determined and then the behaviour of unconfined concrete in the core region will be studied.

The general-purpose finite element program ABAQUS [21] was used to obtain the average confining stress vs. lateral strain curves for the confining tube. Figure 4 shows the plan and elevation of a typical finite element model of a column segment with collars having either bolted or welded corner connections. When the finite element model is loaded in the axial direction, the confining tube is strained laterally due to the dilation of concrete. In response, the confining tube applies confinement stress on to the concrete due to its restraining action. The columns with bolted collars might also exert active confining pressure due to pre-stressing of the bolts. The active confining pressure in the columns with bolted collars was modelled by inducing a negative temperature change in the bolts. Although the confining pressure for columns with bolted collars is a combination of active and passive pressures, the pressure on the columns having collars with welded corner connections is purely passive. It is to be noted from the elevation of the model that an HSS collar has been divided into four layers within the center-to-centre spacing s to represent the equivalent confining tube described above. However, any reasonable number of layers could be selected. The average confinement stress is obtained by dividing the total force in the outriggers located in a strip having a width equal to the column width and a depth equal to the centre-to-centre spacing s of collars, by the strip area. The average lateral strain is obtained by dividing the average horizontal displacements of the concrete surface nodes at which outriggers from the collars are connected, by half the depth of the column. The complete description of the finite element model can be seen elsewhere [22]. The finite element study showed that the collars remain in contact with the column during the majority of the axial load history. Only at very high levels of axial strain may the collar and the concrete at mid-depth of the column break contact. For the practical range of axial strain, it is assumed that the contact between the concrete and the collars remains intact. This assumption has been justified by the testing of the columns in phase one of the project where no gap was observed.

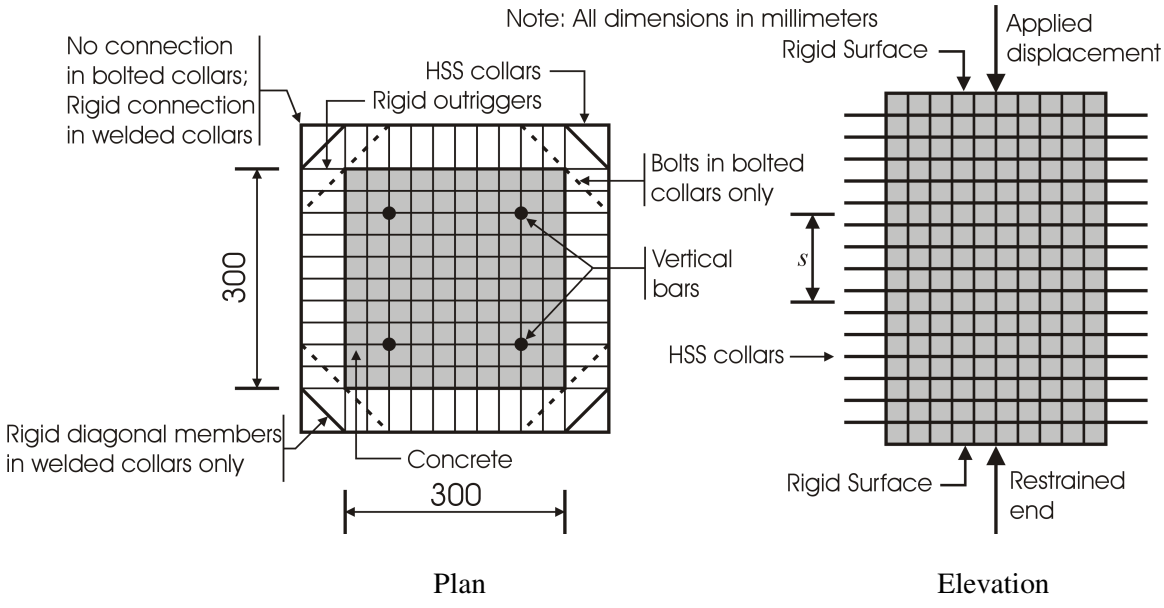

Figure 4: Plan and elevation of a typical finite element model for an externally confined column

It is assumed that the confining behaviour of the collars with welded corners depends on the following primary variables: (1) area of cross-section, A_{collar}, of a side of a collar; (2) moment of inertia, I_{collar}, of a side of a collar about an axis passing through the centroid of the side of the collar parallel to the

longitudinal axis of the column; (3) width, h, of the column; (4) yield stress of the confining steel, f_y; (5) modulus of elasticity, E_s, of the confining steel (taken as a constant equal to 205 000 MPa); (6) confinement stress, σ_{ct}; and (7) lateral strain, ε_l. A dimensional analysis was performed utilizing the Buckingham Pi theorem [23] to identify the following non-dimensional parameters:

$$\beta_1 = \frac{A_{collar}}{A_{column}} \qquad \beta_2 = \frac{I_{collar}}{I_{column}} \qquad \beta_3 = \frac{s}{h}$$

$$\beta_4 = \frac{f_y}{E_s} \qquad \beta_5 = \varepsilon_l \qquad \beta_6 = \frac{\sigma_{ct}}{E_s\left(\frac{f_y}{E_s}\right)^{\frac{2}{3}}}$$

It is to be noted that β_5 and β_6 are output parameters and β_1 to β_4 are input parameters The parameter β_6 did not originally include the parenthetical quantity in the denominator, which was selected through calibration with the finite element results to eliminate the influence of the input parameter β_4. This was deemed advantageous because E_s has been taken as a constant and therefore β_4 cannot be validated directly as an input parameter. This elimination of influence is demonstrated subsequently. By transforming the primary variables to a set of non-dimensional parameters, the scale effects are eliminated from the numerical model and the number of analyses required to control the behaviour of the external confinement are reduced considerably.

Figure 5(a) shows the stress vs. strain curve for an HSS 76x51x6.35 obtained from a stub column test. The Ramberg-Osgood model [24] was calibrated based on this curve. The calibrated model was then used to generate the three material curves depicted in Figure 5(b) for yield stress $f_y = 400$ MPa, $f_y = 500$ MPa, and $f_y = 600$ MPa.

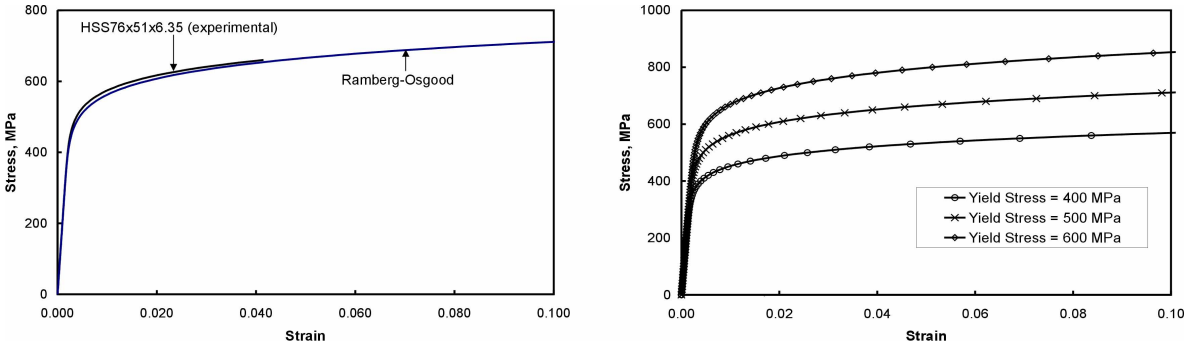

(a) (b)

Figure 5: Stress vs. strain curves of confining steel: (a) calibration of Ramberg-Osgood model; (b) curves generated by the model

The effect of the yield stress of the confining steel on the relationship between β_5 and β_6 was studied with two shapes of the steel material curves: elastic-perfectly plastic and round-shaped as shown in Figure 5(b). Figure 6(a) shows the relationship between β_5 and β_6 for elastic-perfectly plastic confining

steel with yield stress $f_y = 250$ MPa, $f_y = 350$ MPa, $f_y = 400$ MPa, $f_y = 450$ MPa, and $f_y = 500$ MPa. These analyses were carried out using a finite element model with a column cross-section of 300x300 mm and with arbitrarily chosen collars of 20x50 mm solid rectangular cross-section spaced at 25 mm on centres (to approximate the smeared collar condition), oriented to generate maximum flexural stiffness. Figure 6(a) shows that changing the yield stress of the confining steel (and therefore β_4) has no effect on the relationship between β_5 and β_6. This is because of the presence of parameter β_4 in the denominator of parameter β_6. Figure 6(b) shows the relationship between β_5 and β_6 for confining steel with a round-shaped material curve. The objective of this figure is to study the effect of a change of yield stress (and therefore of β_4) and of scale of the various primary dimensional parameters (while keeping the other three non-dimensional input parameters constant) on the relationship between β_5 and β_6.

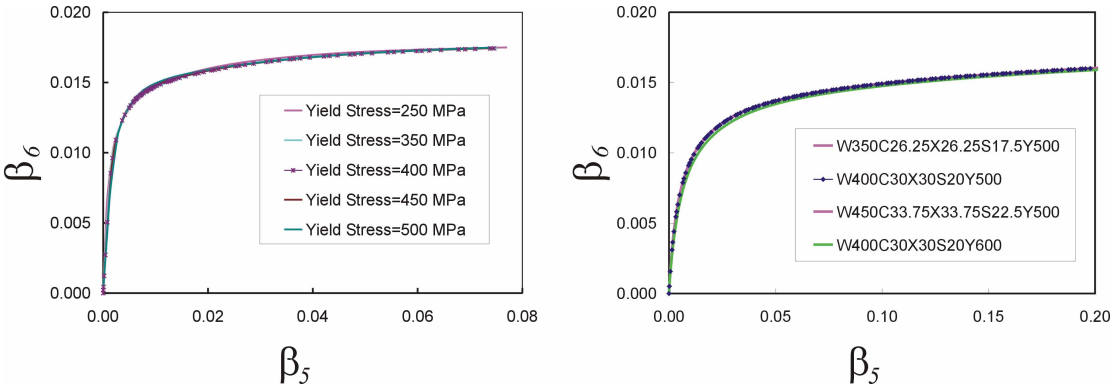

(a) elastic-perfectly plastic steel material curve (b) round-shaped steel material curve

Figure 6: Effect of change of column size and change of yield stress of confining steel on the relationship between parameters β_5 and β_6

To examine the effect of a change of yield stress alone for round-shaped material curves, the results of the models 400x400 mm in cross-section with 30x30 mm collars spaced at 20 mm on centres with yield stresses of 500 MPa and 600 MPa, respectively, can be compared (Figure 6(b)). These curves are identical and hence, the parameter β_4 has also been shown to have no effect on the relationship between the output parameters for the case of round shaped material curves.

The effect of a change in the scale of the model on the relationship between β_5 and β_6 can be studied by comparing the results (Figure 6(b)) obtained from the following models: (1) 350x350 mm in cross-section with collars of 26.25x26.25 mm in cross-section spaced at 17.5 mm on centres; (2) 400x400 mm in cross-section with collars of 30x30 mm in cross-section spaced at 20 mm on centres; and (3) 450x450 mm in cross-section with collars of 33.75x33.75 mm in cross-section spaced at 22.5 mm on centres. All three models have the same values of $\beta_1 = 5.625\text{x}10^{-3}$, $\beta_2 = 3.1641\text{x}10^{-5}$, and $\beta_3 = 5.00\text{x}10^{-2}$, and the same confining steel: round-shaped material curve with a yield stress f_y = 500 MPa and a modulus of elasticity, E_s, equal to 205 000 MPa. The curves (relationship

between β_5 and β_6) from these models overlap each other proving that the non-dimensional parameters (β_1 through β_6) are independent of scale effect.

An investigation is in progress to develop equations for the relationship between β_5 and β_6 in terms of the non-dimensional parameters for the confining tube. Until this study is completed, finite element analysis may be used to determine the this behaviour.

Confined Concrete Curves

Mander *et al*. [8] proposed a model for the stress vs. strain curve of concrete confined by conventional transverse steel reinforcement that assumes constant confining pressure through the axial load history. In this model, the stress vs. strain curve of confined concrete is represented by an equation proposed by Popovics [25] for unconfined concrete. In addition, it utilizes the expression for strain at peak stress of the confined concrete proposed by Richart *et al*. [26] based on the test results of cylinders under constant hydraulic confining pressure. In columns confined externally by HSS collars, the confining pressure varies with the axial load history. Therefore, this model cannot be used directly to predict the stress vs. strain relationships of these columns. However, the model can still be utilized to predict the behaviour of these columns by applying only a small increment of axial strain over which confining pressure can be assumed constant. This leads to an incremental approach to predict the behaviour of externally confined columns similar to that used by Fam and Rizkalla [12] for FRP confinement. During each increment, a different confined concrete material response forms with a different secant modulus of elasticity, $(E_c)_i$, corresponding to a general point *i* on the confined concrete material curve at which the axial strain is $(\varepsilon_{cc})_i$. Similar to the secant modulus of elasticity of concrete, the secant Poisson's ratio, ν_c, also changes with the increase in the axial strain of the column. In addition, the secant Poisson's ratio, ν_c, is also dependent on the magnitude of the confining pressure present in an increment of axial strain. The secant Poisson's ratio in the increment *i* can be represented by $(\nu_c)_i$. Gardner [27] tested concrete cylinders and reported average lateral strain vs. axial strain curves for different confining pressures. Using these results, Fam and Rizkalla [12], developed the following relationship between the secant Poisson's ratio, ν_c, and the axial strain of the confined concrete, ε_{cc}, for different confining pressures:

$$\left(\frac{\nu_c}{\nu_{co}}\right) = C\left(\frac{\varepsilon_{cc}}{\varepsilon'_{cc}}\right) + 1 \qquad [8]$$

The constant *C* (it is considered constant within an increment) was obtained by performing a regression analysis on the experimentally obtained values of *C* at different confining pressures:

$$C = 1.914\left(\frac{\sigma_h}{f'_c}\right) + 0.719 \qquad [9]$$

For increment *i*, Equations 8 and 9 can be written as:

$$\left(\frac{(\nu_c)_i}{\nu_{co}}\right) = (C)_i\left(\frac{(\varepsilon_{cc})_i}{(\varepsilon'_{cc})_i}\right) + 1 \qquad [10]$$

$$(C)_i = 1.914\left[\frac{(\sigma_h)_i}{f'_c}\right] + 0.719 \quad [11]$$

Knowing $(\varepsilon_{cc})_i$ and $(\nu_c)_i$ in an increment *i*, the lateral strain $(\varepsilon_l)_i$ in the increment can be calculated as:

$$(\varepsilon_l)_i = (\nu_c)_i (\varepsilon_{cc})_i \quad [12]$$

Knowing $(\varepsilon_l)_i$, the confinement stress, $(\sigma_{ct})_i$, can be found from the relationship between the confinement stress vs. lateral strain (similar to Figure 2) obtained from the finite element analysis. Then $(E_{ct})_i$ can be calculated as:

$$(E_{ct})_i = \frac{(\sigma_{ct})_i}{(\varepsilon_l)_i} \quad [13]$$

The confining pressure $(\sigma_h)_i$ due to collar confinement in increment *i* can be calculated from the following equation, the derivation of which has been given before:

$$(\sigma_h)_i = \frac{(\nu_c)_i}{\frac{1}{(E_{ct})_i} + \frac{1-(\nu)_i}{(E_c)_i}} (\varepsilon_{cc})_i \quad [14]$$

If there exists active confining pressure in addition to passive confining pressure, the above equation is not applied to the active confining pressure. In that case, the total confining pressure in the increment *i* will become $(\sigma_h)_i$ plus the active confining pressure.

Knowing $(\sigma_h)_i$ in an increment *i*, the peak stress of the confined concrete $(f'_{cc})_i$ can be determined from the following equation which is also used by Mander *et al*. [8]:

$$(f'_{cc})_i = f'_c\left[2.254\sqrt{1+\frac{7.94(\sigma_h)_i}{f'_c}} - 2\frac{(\sigma_h)_i}{f'_c} - 1.254\right] \quad [15]$$

Then, the strain at peak stress, $(\varepsilon'_{cc})_i$, of the confined concrete material can be determined from the following equation (Richart *et al*. [26]):

$$(\varepsilon'_{cc})_i = \varepsilon_{co}\left[1 + 5\left(\frac{(f'_{cc})_i}{f'_c} - 1\right)\right] \quad [16]$$

Then, according to Mander *et al.* [8], the Popovics [25] equation is utilized to determine the confined concrete stress, $(f_{cc})_i$, at axial strain $(\varepsilon_{cc})_i$ as given below:

$$(f_{cc})_i = \frac{(f'_{cc})_i (x)_i (r)_i}{(r)_i - 1 + (x)_i^{(r)_i}} \quad [17]$$

where:

$$(r)_i = \left[\frac{E_{co}}{E_{co} - (E_{sec})_i} \right] \quad [18]$$

$$(E_{sec})_i = \frac{(f'_{cc})_i}{(\varepsilon'_{cc})_i} \quad [19]$$

$$(x)_i = \frac{(\varepsilon_{cc})_i}{(\varepsilon'_{cc})_i} \quad [20]$$

Knowing the stress of confined concrete $(f_{cc})_i$ at strain $(\varepsilon_{cc})_i$, the secant modulus of elasticity, $(E_c)_i$, in increment *i* can be calculated as:

$$(E_c)_i = \frac{(f_{cc})_i}{(\varepsilon_{cc})_i} \quad [21]$$

Several unknowns are encountered in a particular increment on the axial strain of the confined concrete. Hence, the method of successive approximations is used on Equations 10 to 21 to converge to the solution within each increment. For example, for a particular level of axial strain of concrete in *i*th increment, $(\varepsilon_{cc})_i$, the secant modulus of elasticity, $(E_c)_i$, the secant Poisson's ratio, $(\nu_c)_i$, the constant $(C)_i$, the strain at peak stress of confined concrete, $(\varepsilon'_{cc})_i$, the secant slope, $(E_{ct})_i$, of the behavioural curve of the confining tube, and the confining pressure, $(\sigma_h)_i$, are unknown. The values of these unknowns are assumed arbitrarily in the first iteration in an increment. In subsequent iterations in the same increment, the values from the immediately previous iteration are used. Iterations are performed until the values of these variables converge. Then, the next increment in axial strain of the confined is taken and the process is repeated. In this way, the stress vs. strain curve of externally confined concrete is traced until some failure criterion is met. This process of tracing the confined material curve is path-independent because we can find the confined concrete stress, $(f_{cc})_i$, at any level of strain, $(\varepsilon_{cc})_i$, in an increment *i* without knowing the trace of confined concrete material curves in the previous increments.

Behaviour of Unconfined Core Concrete

Some portion of the concrete in the core of the externally confined column is effectively unconfined. The depth of this unconfined concrete into the core was determined based on tests of externally confined

columns under concentric axial loading conducted at the University of Alberta. The average depth of parabolic concrete spalling between the collars at the peak load was found to be $0.29\,s'$, which is higher than the depth of concrete spalling between ties equal to $0.21\,s'$ reported by Chung *et al*. [11] based on analytical derivations, where s' is the clear spacing between the collars or ties. To simulate the behaviour of cover concrete, the following expression was proposed by Muto [28]:

$$f_c = 6.75 f_c'(e^{-0.812\xi} - e^{-1.218\xi}) \qquad [22]$$

where $\xi = \varepsilon_c / \varepsilon_s$, f_c and ε_c are stress and strain of unconfined concrete, and ε_s is the strain at which spalling of the unconfined concrete starts. The same expression is adopted to represent the behaviour of the parabolic concrete region between the collars in externally confined columns. Muto [28] took ε_s equal to the strain at peak stress of the unconfined concrete. For externally confined columns, it is recommended that ε_s be taken equal to the average of experimentally observed strains at which concrete spalling started based on externally confined columns tested under concentric axial loading [22]. The average value of this strain was found to be 0.0039.

Application of the Proposed Model

The proposed model was applied to columns C01, C06, CL1, and CL5. Columns C01 and C06 were tested under concentric axial load and columns CL1 and CL05 were tested under lateral cyclic loading without gravity load. The detail of these columns and the corresponding measured material properties can be seen in reference [14]. The strength of concrete in a column is generally lower than the measured cylinder strength because of the differences in size, shape, and casting method used for standard cylinders and the column specimen. In the present study, it is assumed that the strength of the concrete in the column is 85% of the concrete strength obtained from the standard cylinders. The secant modulus of elasticity, E_c, of the concrete is taken equal to $3700\sqrt{f_{co}'}$. A well-known relation—two times the concrete strength of columns, f_{co}', divided by E_c—is used to estimate the strain at peak stress, ε_{co}, of the unconfined column concrete.

Figure 7(a) shows the confining pressure vs. lateral strain relationships obtained by finite element analyses. Using the proposed procedure, the stress vs. strain curves of confined concrete in the core are obtained, as shown in Figure 7(b). Figure 7(c) shows the behaviour of unconfined concrete in the core modelled by Equation [22] for these columns. The total column load vs. axial strain relationships are obtained by summing the load vs. strain curves of vertical rebars, confined concrete in the core, and unconfined concrete in the core. Figure 7(d) shows the load vs. strain curves for columns C01 and C06 obtained analytically and experimentally. The experimental and analytical curves are close to each other up to an axial strain of at least 0.03. After this level of axial strain, the experimental and analytical curves begin to diverge. This discrepancy is related to the bending of vertical bars, which is not considered in the proposed model. Similarly, the load vs. strain curves were obtained for columns CL1 and CL5 tested under horizontal cyclic loading without gravity load (Figure 7(e)). No experimental load vs. strain curves are available for these columns for comparison. Figure 7(f) shows the confined concrete material curves based on the core area of the collared columns. The ordinates of these curves were obtained by dividing the total load carried by the confined and unconfined concrete in the core at a specific level of axial strain, by the core area of the columns, which is equal to the gross area of the collared columns.

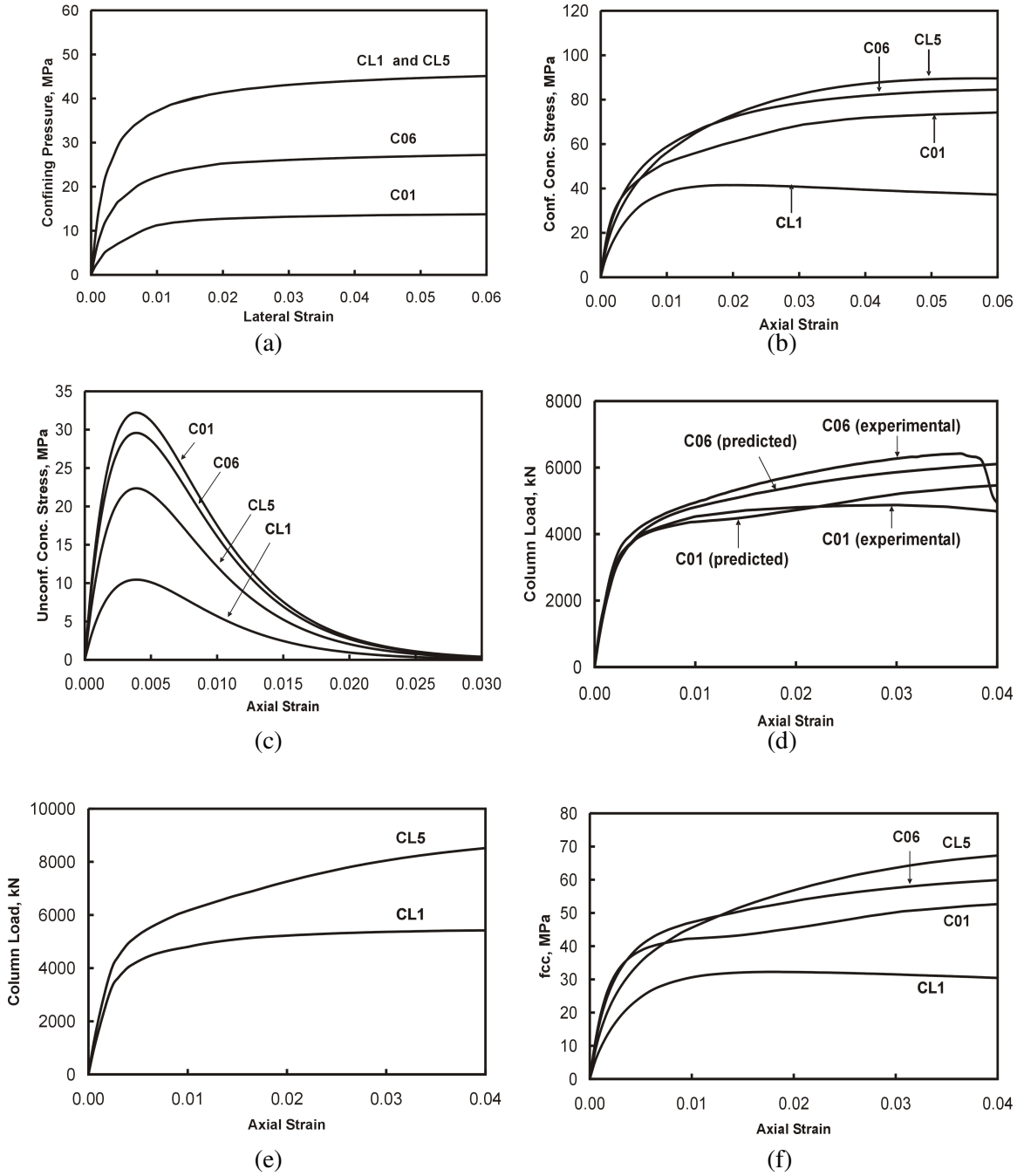

Figure 7: Development of confined concrete material curves

MODELLING OF PLASTIC HINGES

The horizontal displacement of a cantilever column at the point of application of the horizontal load consists of flexural deformations, shear deformations, deformations due to the rotation of the column at the footing resulting from the extension of reinforcement within the anchorage zone of the footing, and displacement due to sliding of the column over the footing. The bond between the vertical reinforcement and the footing concrete in the anchorage zone, as well as the column concrete near the footing, breaks

due to the bar elongation. Saatcioglu and Ozcebe [29] found that deformations due to shear and reinforcement elongation both increase with an increase in inelastic strain of the columns.

The horizontal displacement at the point of application of horizontal load due to flexure (including both the elastic and inelastic components) can be calculated by the following equation proposed by Park and Paulay [30]:

$$\Delta = \left(\frac{\phi_y L^2}{3} \right) + \left(\phi - \phi_y \right) L_p \left(L - \frac{L_p}{2} \right) \qquad [23]$$

where Δ is the lateral displacement of the column at the point of application of the horizontal load, L is the height of the column from the base to the point of load application, L_p is the plastic hinge length, ϕ_y is the yield curvature, and ϕ is the curvature at a general level of lateral displacement. A detailed investigation of the collared columns tested under simulated seismic loading is underway to determine the plastic hinge lengths. In the present paper, an expression proposed by Mattock [31], *i.e.*, $L_p = 0.05L + 0.5d$, is used to calculate the plastic hinge lengths of the collared columns, where *d* is the effective depth of the section. Within the hinge region, the curvature is assumed uniform, while a linearly distributed curvature is assumed in the upper portion of the column (*i.e.*, outside of the hinge region).

The rotation at the base of the column can be estimated by multiplying the curvature by the distance L_b, where L_b is the length of vertical reinforcement over which debonding takes place [32]. The displacement at the point of application of horizontal load can be calculated by multiplying the base rotation by the height L.

The shear deformations and sliding of the column over the footing also contribute to the horizontal displacement of the columns at the point of application of horizontal load. However, their contribution is less significant as compared to flexural deformations and deformations due to the rotation of the column at the base resulting from the extension of vertical reinforcement. Moreover, the shear deformations and sliding at the footing are less significant in columns with a long shear span as compared to columns with a short shear span.

In order to apply the above procedure to determine lateral drift at the point of application of horizontal load, the moment vs. curvature relationships are required which can be determined using strain compatibility analysis. The procedure was applied to two columns: CL1 and CL5. These columns were tested with a long and a short shear span, respectively, without gravity load. The confined concrete material curves for these columns are given in Figure 7(f). It is to be noted from these curves that a failure criterion has not yet been defined and hence, the curves do not descend at large strains. Therefore, it is expected that the predicted envelope curves will overestimate the column capacity at high levels of lateral drift. The moment vs. curvature relationships for columns CL1 and CL5 are given in Figures 8(a) and 8(b), respectively. The effect of the strain gradient on the stress vs. strain curves of confined concrete was ignored while establishing these relationships. The failure criterion of the stress vs. strain curves of confined concrete are currently in the process of being defined in terms of the non-dimensional parameters described in the previous section.

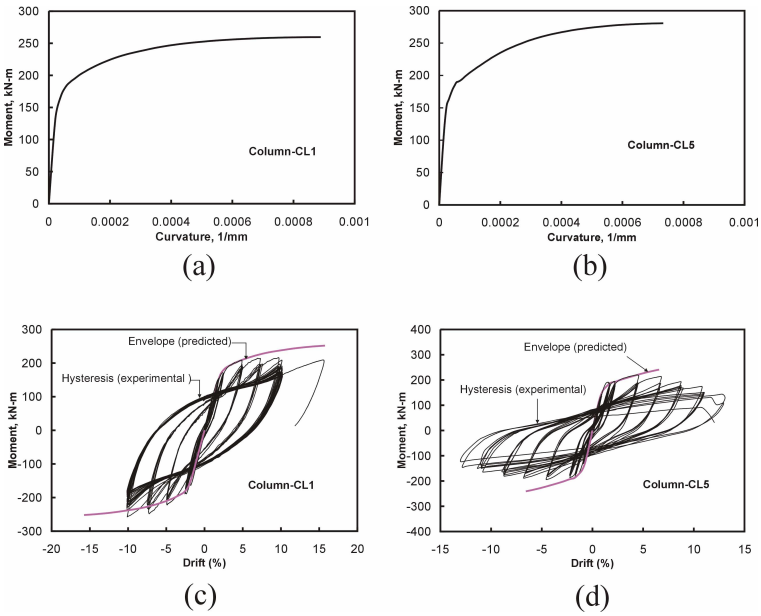

Figure 8: (a,b) Moment vs. curvature relationships; (c,d) moment vs. lateral drift hysteresis and predicted moment lateral drift envelope curves

Figure 8(c) shows the experimental moment vs. lateral drift hysteresis and the analytical envelope curve for column CL1. The analytical envelope curve includes the effect of flexural deformations and deformations due to the rotation of the column at the base due to the extension of reinforcement in the anchorage zone. The sliding and shear deformations were ignored because of the large shear span of this column. Considering the asymmetry of the experimental hysteresis curve, the predicted envelope shows very good agreement with the experimental curve up to a lateral drift of about 10%. The rotation at the base due to the extension of rebars in the anchorage zone was estimated by multiplying the curvature by the distance L_b. Harmon *et al.* [32] found L_b equal to $9d_b$ through calibration with test results for FRP confined columns. Because of the nature of collar confinement, L_b is assumed equal to $4d_b$ for columns CL1 and CL5. In both cases, the clear spacing between collars was 50 mm, so there was a 25 mm clear space between the footing and the first collar. The value selected for L_b accounts for debonding of the bar in this space with a slight penetration under the first collar, plus debonding within the depth of the cover concrete in the footing to the bottom of the top footing bars. This unbonded length is supported by observations made during the testing programme. However, when the procedure will be applied to all the columns tested under simulated cyclic loading, a slight variation in this assumption is expected to account for differences in the efficiency of confinement for different collar arrangements.

Figure 8(d) shows the experimental hysteresis curve and the predicted envelope curve for column CL5. The predicted envelope curve includes the effect of flexural deformations, rotation at the base, and the experimentally obtained sliding of the column at the top of the footing. However, the sliding was small compared to the deformations related to flexure and base rotation. The contribution of shear deformations was also ignored in this case because no shear distress was observed in the column during testing. The effect of shear deformations will be included in future studies for columns with short shear spans, however, it is anticipated that the shear deformations will be relatively small. The predicted curve shows very good agreement with the experimental curve up to a lateral drift of about 5%. The degradation in strength due to cyclic loading is more severe in columns with short shear spans, as compared to those with long shear spans, as is clear from the hysteresis curves of columns CL1 and CL5. Figure 9 shows the

base rotations of columns CL1 and CL5 at the end of the tests. The extension and rupture of the vertical rebars of column CL5 are evident in Figure 9(b).

(a) Column CL1 (b) Column CL5

Figure 9: Rotation of columns CL1 and CL5 at the base

SUMMARY AND CONCLUSIONS

A stress–strain model for concrete in columns confined externally by steel hollow structural sections (HSS) is proposed. The model takes into account the flexural as well as axial stiffnesses of the collars. The confined concrete material curves predicted by the model show very good agreement with the material curves of the confined concrete obtained experimentally. To control the behaviour of HSS collar confinement, six non-dimensional parameters have been identified and validated. The descending branch of the model is under development in terms of the non-dimensional parameters.

The moment–curvature relationships were developed using strain compatibility analysis utilizing the confined concrete material curves obtained from the proposed model and measured stress–strain curves of the longitudinal steel. The horizontal displacement at the point of horizontal load is assumed to consist of elastic deformation in the columns, plastic rotation at the base hinge, rotation at the base of the column due to the elongation and debonding of the longitudinal reinforcement close to the column/footing interface, shear deformations, and sliding of the column at the base. However, the contributions to the horizontal displacement of shear deformations and sliding at the base are less significant as compared to the contributions of rotation in the plastic hinge region and the rotation at the base. The predicted envelope curves show very good agreement with the experimentally obtained hysteresis curves in the low and moderate ranges of lateral drift. However, in the higher range of lateral drift, the predicted curves overestimate the column capacity due to the lack of a descending branch in the confined material curve, which is still under development.

ACKNOWLEDGEMENTS

The funding for this project was provided by the Natural Sciences and Engineering Research Council of Canada. The authors are grateful to Reliable Tubes Ltd., Unicon Concrete Ltd., and Master Builders for their donations in carrying out this project and to the Centre for Engineering Research, Edmonton, Canada, who provided the test facility for two of the columns in the research programme.

NOTATION

d = effective depth of the section, mm;

E_c = secant modulus of elasticity of unconfined concrete, MPa;

$(E_c)_i$ = slope of an ith secant line corresponding to a general point *i* on the confined concrete material curve; $(E_c)_i = \dfrac{(f_{cc})_i}{(\varepsilon_{cc})_i}$, MPa;

$(E_{ct})_i$ = slope of an *i*th secant line to a general point *i* on the behavioural curve of the confining tube; $(E_{ct})_i = \dfrac{(\sigma_{ct})_i}{(\varepsilon_l)_i}$, MPa;

E_{co} = initial tangent modulus of elasticity of unconfined concrete, MPa;

E_s = modulus of elasticity of steel, MPa;

f'_c = compressive strength of concrete based on standard cylinders, MPa;

f'_{co} = compressive strength of unconfined concrete in the column, MPa;

f_c = stress of unconfined concrete at a general axial strain, MPa;

f_{cc} = stress of confined concrete, MPa;

$(f_{cc})_i$ = stress of confined concrete corresponding to a general point *i* on the confined concrete material curve, MPa;

f_y = yield strength of steel, MPa;

L_b = length of vertical reinforcement over which debonding takes place, MPa;

L_p = plastic hinge length, MPa;

σ_{ct} = average confinement stress of the confining tube, MPa;

σ_h = average confining pressure, MPa;

s = center-to-center spacing of ties or collars, mm;

s' = clear spacing between the collars, mm;

$(\varepsilon_{cc})_i$ = axial strain of confined concrete corresponding to a general point *i* on the confined concrete material curve;

ε'_{cc} = strain at peak stress of confined concrete under constant confining pressure;

ε_s = strain at which spalling of concrete starts during axial load history;

β_1 to β_6 = non-dimensional behavioural parameters of confining tube;

ν_c = secant Poisson's ratio of concrete at a given level of axial strain;

ν_{co} = initial secant Poisson's ratio of concrete;

ϕ = curvature at a general level of deformation;

ϕ_y = yield curvature;

REFERENCES

1. Iyengar, K.T.S.R, Desayi, P., and Reddy, K.N., "Stress-strain characteristics of concrete confined in steel binders," Magazine of Concrete Research, 1970, 22(22): 173-184.
2. Vallenas, J., Bertero, V.V., and Popov, E.P., "Concrete confined by rectangular hoops subjected to axial loads," Report 77/13, Earthquake Engineering Research Centre, University of California, Berkeley, CA, 1977.
3. Sheikh, S.A. and Uzumeri, S.M., "Strength and ductility of tied concrete columns," Journal of the Structural Division, ASCE, 1980, 106(ST5): 1079-1102.
4. Scott, B.D., Park, R., and Priestley, M.J.N., "Stress-strain behaviour of concrete confined by overlapping hoops at low and high strain rates," ACI Journal, 1982, 79: 13-27.
5. Mander, J.B., Priestley, M.J.N. and Park, R., "Observed stress-strain behavior of confined concrete," Journal of Structural Engineering, ASCE, 1988, 114(8): 1827-1849.
6. Kent, D.C. and Park, R., "Flexural members with confined concrete," Journal of the Structural Division, ASCE, 1971, 97(ST7): 1969-1990.
7. Sheikh, S.A. and Uzumeri, S.M., "Analytical model for concrete confinement in tied columns," Journal of the Structural Division, ASCE, 1982, 108(ST12): 2703-2722.
8. Mander, J.B., Priestley, M.J.N. and Park, R., "Theoretical stress-strain model for confined concrete," Journal of Structural Engineering, ASCE, 1988, 114(8): 1804-1826.
9. Saatcioglu, M. and Razvi, S.R., "Strength and ductility of confined concrete," Journal of Structural Engineering, ASCE, 1992, 118(6): 1590-1607.
10. Légeron, F., and Paultre, P., "Uniaxial confinement model for normal- and high-strength concrete columns," Journal of Structural Engineering, ASCE, 2003, 129(2): 241-252.
11. Chung, H., Yang, K., Lee, Y., and Eun, H, "Stress-strain curve of laterally confined concrete," Engineering Structures, 2002, 24: 1153-1163.
12. Fam, A.Z. and Rizkalla, S.H., "Confinement models for axially loaded concrete confined by circular fiber-reinforced polymer tubes," 2001, *ACI Structural Journal, 2001,* 98 (4): 451-461.
13. Samaan, M., Mirmiran, A. and Shahawy, M., "Model of concrete confined by fiber composites," *Journal of Structural Engineering,* ASCE*, 1998,*124(9): 1025-1031.
14. Hussain, M.A., and Driver, R.G., "Experimental study on the seismic performance of externally confined reinforced concrete columns," Paper No. 578, Proc., 13th World Conference on Earthquake Engineering, Vancouver, BC, Canada, August 1-6, 2004.
15. Hussain, M.A., and Driver, R.G. (2001). "Finite element study on the strength and ductility of externally confined rectangular and square concrete columns," 29th Annual Conference of Canadian Society for Civil Engineering, Victoria, B. C., Canada, May 30-June 2.
16. Khaloo, A.R., and Bozorgzadeh, A., "Influence of confining hoop flexural stiffness on behavior of high-strength lightweight concrete columns," ACI Structural Journal, 2001, 98(5): 657-664.
17. Ghobara, A., Aziz, S.T., and Biddah, A., "Rehabilitation of reinforced concrete frame connections using corrugated steel jacketing," ACI Structural Journal, V. 4, No. 3, May-June 1997, pp. 283-291.
18. Xiao, Y., and Wu, H., "Retrofit of reinforced concrete columns using partially stiffened steel jackets," Journal of Structural Engineering, ASCE, V. 129, No. 6, May-June 2003, pp. 725-732.
19. Caner, F.C. and Bažant, Z.P., "Lateral confinement needed to suppress softening of concrete in compression," Journal of Engineering Mechanics, ASCE, V. 128, No. 12, December 1, 2002, pp. 1304-1313.
20. Young, W.C., "Roark's formulas for stress and strain," Sixth Edition, McGraw-Hill, Inc., 1989: 832 pp.
21. ABAQUS/Standard user's manual, Hibbitt, Karlsson & Sorensen, Pawtucket, R.I., 2003.
22. Hussain, M.A., and Driver, R.G., "Finite element analysis of reinforced concrete columns seismically upgraded by external collar confinement," Proc., Extreme Loading Conference, Toronto, Ontario, Canada, August 3-6, 2003.
23. Langhaar, H.L., "Dimensional analysis and theory of models," John Wiley and Sons, N.Y., 1951.

24. Chen, W.F. and Han, D.J., “Plasticity in structural engineering,” Springer-Verlag, 1988.
25. Popovics, S, “A numerical approach to the complete stress-strain curve of concrete,” Cement and Concrete Research, Pergamon Press, Inc., 1973, (3): 583-599.
26. Richart, F.E., Brandtzaeg, A., and Brown, R.L., “ A study of the failure of concrete under combined compressive stresses,” University of Illinois Engineering Experimental Station, Bulletin No. 185, 1928: 104 pp.
27. Gardner, N.J., “Triaxial behaviour of concrete,” ACI Journal, 1969: 136-146.
28. Muto, C., “Seismic design series—the plastic design of reinforced concrete structures,” in Japanese, 1974.
29. Saatcioglu, M. and Ozcebe, G., “Response of reinforced concrete columns to simulated seismic loading,” ACI Structural Journal, 1989: 3-12.
30. Park, R. and Paulay, T., “Reinforced concrete structures,” John Wiley & Sons, 1975.
31. Mattock, A.H., “Discussion of “Rotational Capacity of Reinforced Concrete Beams” by Corley W.G.,” Journal of Structural Division, ASCE, 1967, 93(ST2): 519-522.
32. Harmon, T.G., Gould, N.C., Ramakrishnan, S., and Wang, E.H., “Confined concrete columns subjected to axial load, cyclic shear, and cyclic flexure—Part I: analytical models,” ACI Structural Journal, 2002, 99(1): 32-41.